Gymnasium Illumination Measurement Method Research based on UAV

Shengwei Jia[1,a], Nianyu Zou[1,b*], Songhai Xu[1,c]

jsw15212021@163.com[a], n_y_zou@dlpu.edu.cn[b*], xvsonghai@163.com[c]

Research Institute of Photonics, Dalian Polytechnic University, Dalian 116034, China[1]

Abstract: Stadium illumination is an important standard of the light environment when stadiums host major sporting events and broadcast sports. The rules of stadium illumination are strict and complex, and there are wide measuring ranges and variable measurement environments in different sports events. For fast and accurate acquisition of stadium illumination in different environments, in this paper, a micro control module for collecting illumination has been designed which is based on the STM32F103RCT6, and in the following work, the module is combined with the UAV because of the convenience of the function of the fight. According to the optical flow positioning function of UAV, the position information can be shown on the mobile application. We set up simulated experimental scenarios for illumination acquisition, and the system can transmit data to the OneNET cloud platform in 5-second intervals verified by experiments. Besides, changes in illumination data can be displayed in real-time on the cloud platform. Meanwhile, the Least Square Method is used as an algorithm for data processing to eliminate errors.

Keywords: gymnasium illumination, measuring systems, UAV, IoT

1 INTRODUCTION

As our economy develops and our international status increases, we are hosting more and more international sporting events. And in recent years, China's sports industry has grown even more. Meanwhile, large stadiums and professional stadiums are becoming more and more well-built as people become more fitness conscious. Therefore, the illumination requirements are more stringent and complex. As early as the 2008 Olympic Games, the BOB (Beijing Olympic Broadcast Board) set the most stringent lighting requirements for the Bird's Nest National Stadium in order to meet the needs of athletes, spectators, and broadcasters, which includes requirements for the vertical illuminance, the illuminance gradients, the four-sided direct illuminance ratios, etc. (Yao 2012). In particular, stadiums with event broadcast needs have clear requirements for vertical illumination in the direction of the primary camera and vertical illumination in the direction of the secondary camera (Li 2020), which makes illuminance measurement more complex and rigorous. In order to achieve the needs of good competition and broadcasting, the Standard for the Design and Inspection of Stadium Lighting (JGJ153-2016) (abbreviated the Standard) classifies the sports lighting levels into six classes. Comprehensive stadiums are generally rated above IV in terms of venue lighting due to the need to accommodate a variety of competition events and the existence of broadcast demand for most games nowadays (Yu 2019). In the face of the above-mentioned situations, it is time and labor-intensive to measure the illuminance distribution in sports stadiums using the application of

EMIS 2023, February 24-26, Chengdu, People's Republic of China

DOI 10.4108/eai.24-2-2023.2330675

traditional illuminance meters.

With the development of science and technology, in the 1990s, research on multi-rotor UAVs continued to break through against the backdrop of the growing maturity of microelectromechanical systems and microsensor technology. The use of UAVs is also becoming more widespread. For example, Takaya Maemura and others at Kobe University, Japan, used a PHANTOM4 drone with an illuminance sensor to obtain data and map the vertical and horizontal illuminance distribution on different planes of the stadium to investigate how to get a detailed picture of the light flow in a large space (Maemura 2017). Traditional UAVs on the market mainly achieve their own positioning through GPS. In recent years, thanks to vision-based indoor positioning technology, UAVs have been able to achieve accurate positioning even in scenarios without GPS, further expanding the application scenarios of UAVs. Ao Ruigui, who is from the Dalian University of Technology, proposed the research on water quality detection method based on UAV multispectral point cloud data and MGGP artificial intelligence algorithm (Ao 2021). They used the flight characteristics of UAVs to take multispectral images and obtain point clouds of suspended matter concentrations using a multispectral camera on board the drone. It is clear that the use of UAVs has expanded into a wide range of industries.

Considering the problems of illumination measurement in large stadiums and the growing use of drones and their extreme convenience. This paper proposes the design of a UAV-based illumination acquisition system. In previous studies, measurement methods for UAV-mounted sensors were not well automated, we combine the convenience of flying a UAV with the STM32 microcontroller to design an illuminance measurement system that obtains the location of measurement points through the UAV's own attitude resolution and displays the data in real-time via an IoT platform, providing a convenient method for illuminance measurement in stadiums.

2 ILLUMINATION STANDARD

In stadiums used to host and televise major sporting events, the illumination requirements generally need to meet the requirements of the players, the spectators and the televisions (Zhao 2019). The Standard specifies the vertical illuminance in the direction of the main camera and the vertical illuminance in the direction of the secondary camera in order to meet the broadcasting needs of some stadiums, in addition to the common illuminance parameters such as horizontal illuminance and vertical illuminance. And the stadium lighting is divided into different grades according to the actual function of the stadium. The ratio of horizontal minimum to maximum illuminance is 0.3 and the ratio of horizontal minimum to average illuminance is 0.7 for Class IV stadiums that can meet basic broadcast needs. Besides, the vertical illumination in the direction of the main camera should be 1000lx, the ratio of minimum to maximum illuminance is 0.4 and the ratio of minimum to average illuminance is 0.6; Vertical illumination in the direction of the auxiliary camera should be 750lx, The ratio of minimum to maximum illuminance is 0.3 and the ratio of minimum to average illuminance is 0.5. When dealing with higher-level stadiums, the requirements for illumination are even higher. In stadium illuminance measurements, horizontal and vertical illuminance are usually measured according to the center point method.

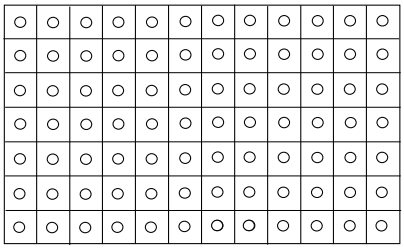

Fig. 1 Schematic diagram of illuminance measurement by the center point method

As shown in Figure 1, it is specified that when performing horizontal illuminance measurements by the center point method, the measurement points should be arranged at the center point of each grid. The measuring equipment should be placed flat on a level surface above the site and the personnel present must be kept away from the measuring equipment during the measurement.

And the vertical illumination of the primary and secondary cameras needs to be measured in stadiums with broadcast requirements. When measuring the vertical illuminance of the main camera, a height of 1.5m is desirable and the normal direction of the photoelectric receiving surface of the measuring equipment should be aligned with the optical axis of the camera lens. During the vertical illuminance measurement of the auxiliary camera, a height of 1m is required and the illuminance on the vertical ground parallel to the four side lines is measured.

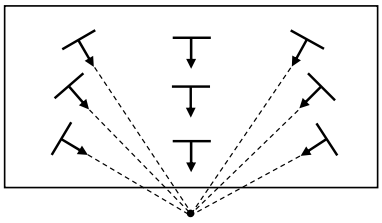

Fig. 2 Schematic diagram of the main camera vertical illumination test

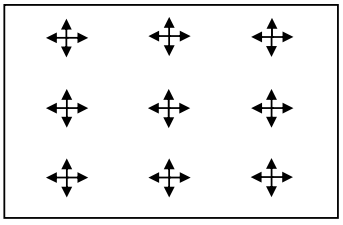

Fig. 3 Schematic diagram of the auxiliary camera vertical illumination test

The main camera and auxiliary camera illumination measurement diagrams are shown in Figure 2 and Figure 3. Besides, in the illumination requirements of the swimming pool, the specific area directly in front of the diving platform and diving board should be made to meet the vertical illumination requirements and the 2m area around the pool should meet the vertical illumination requirements. As you can see, the illuminance requirements for stadiums are strict and complex, but most of the illuminance measurements for stadiums today are still carried out manually, and the measurement process is often labor-intensive and time-consuming.

3 SYSTEM CONSTRUCTION

The measurement system proposed in this paper consists of two main parts, one is the illuminance acquisition module with STM32F103RCT6 as the core, GY-30 as the illuminance sensor and ESP8266 as the wireless data transmission; the other part is the UAV platform carrying the illuminance acquisition module and obtaining the location information. And the system can transmit the processed data to the OneNET cloud platform via the WIFI module. The overall system architecture is shown in Figure 4.

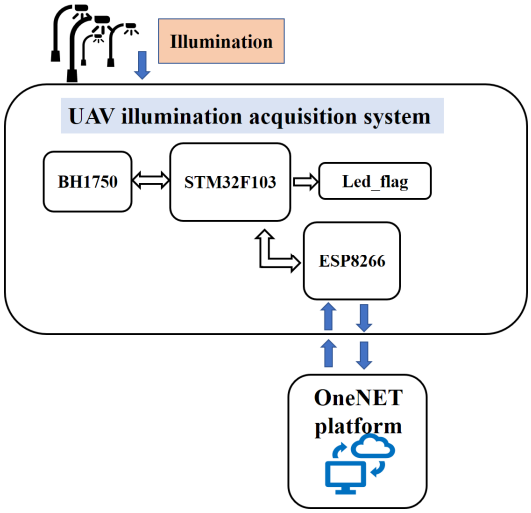

Fig. 4 Schematic diagram of the system architecture

3.1 System hardware design

In this paper, the STM32F103RCT6 was selected as the data processing module for the illumination acquisition module. The chip is produced with the Cortex-M3 core by STMicroelectronics and features high speed and low power consumption. And it is widely used in all aspects of power electronic systems and its small size and light weight make it suitable for carrying on board unmanned aircraft. The GY-30 illuminance sensor has been selected as the sensor for illuminance acquisition with peripheral circuitry such as the BH1750FVI chip and 16bit AD converter, so it has a direct digital output. Meanwhile, the GY-30 can also collect illumination information at 100ms intervals with an accuracy of 1lx. In addition, since the human eye produces different visual intensities for different visions, the visible wavelength range of the human eye is 400nm-760nm, and therefore a visual function V(λ) is defined in photometry to represent the sensitivity of the human eye to different wavelengths of light. As there are certain differences in the visual function of different people in different environments, the International Commission on Illumination (CIE) has also set international standards for the visual function for the sake of uniformity. The human eye elicits the strongest visual response to light at a wavelength of 555nm, and the standard defines the value of the visual function at this point as 1, i.e. v(555) = 1. The illuminance sensor chosen for this paper also takes this characteristic into account, with a built-in photodiode that responds to the spectrum in a manner

close to that of the human eye. A comparison of the GY-30 spectral response curve with the human eye spectral response curve is shown in Figure 5.

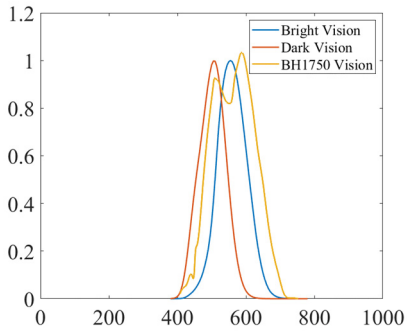

Figure.5 BH1750 spectral response curve and human eye spectral response curve

As shown in Figure 5, the horizontal axis represents the wavelength of light and the vertical axis represents the value of the visual function in the change curve of the visual function. The blue curve represents the visual function curve of the human eye in a bright environment, the red curve represents the visual function curve of the human eye in a dim environment and the yellow curve represents the response curve of the GY-30 to different wavelengths of light. The change in curve shows that the illuminance sensor chip has a similar sensitivity to wavelengths of light as the human eye. when there is light oblique to the illuminance sensor, any radiation source in the unit stereo angle out of the radiation intensity is proportional to the direction of emission and the cosine of the angle normal to the irradiated surface according to Lambert's law. However, in the actual measurement process, the light is refracted by the sensor and the surrounding structures can block the light, resulting in a loss of energy from the incident light. So, it is often necessary to add a cosine corrector to correct for this error. The cosine corrector is made of a diffuse transmitting material so that when the incident light is transmitted through it, the sensor chip receives diffuse light regardless of the angle at which the incident light hits the cosine corrector. The cosine corrector is available in four shapes, including flat, dish, spherical, and planar shapes, and their cosine correction results at different angles are shown in Table 1.

Table 1: Comparison of correction results for different shape cosine correctors

shape	10°	30°	50°	70°	80°
flat	-2.5%	-10%	-15%	-55%	-
dish	-	-3%	-	-	-
spherical	0	0	0	0	-
planar	<0.1%	0.3%	<1%	-	<10%

As shown in Table 1, combining the correction effects of each shape cosine corrector in the table, the spherical shell cosine corrector is chosen for the illumination acquisition system proposed in this paper.

Data transfer between the various modules of the illumination acquisition system is done via a defined communication protocol. Data is transferred between the illuminance sensor and the STM32F103RCT6 core processor via the I2C communication protocol, in which the I2C bus communication protocol is a serial, synchronous communication protocol that communicates between chips via the SCL (serial clock line) and SDA (serial data line). The STM32F103RCT6 microcontroller then processes the data from the illumination sensor and transmits it wirelessly via WiFi to the IoT cloud platform. In this paper, ESP8266-01s is selected as the wireless WiFi communication module, which is small, stable and has a built-in PCB on board antenna. WiFi as a wireless LAN technology based on the IEEE standard, while communication distances of up to one hundred meters can be achieved. And with the development of science and technology more and more campuses and cities have achieved full WiFi coverage, in addition, the low power consumption of WiFi for data transmission facilitates the choice of power supply for the illumination acquisition system for later deployment on the UAV platform. The ESP8266-01s selected for this paper implement data transfer with the STM32F103RCT6 microcontroller via serial communication (UART), in which serial communication is an asynchronous, serial method, and both the STM32 microcontroller and the ESP8266 module have universal synchronous asynchronous transceivers for serial communication with each other. The hardware architecture of the illuminance acquisition module is shown in Figure 6.

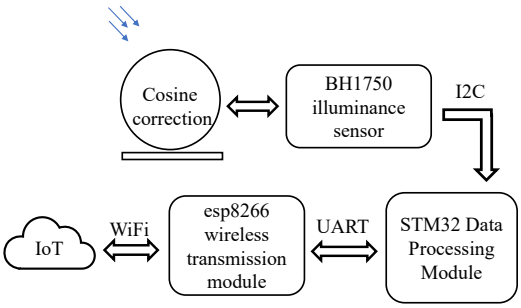

Fig. 6 Hardware structure of the illuminance acquisition module

3.2 System software design

The system proposed in this paper uses the Keil uVision5 integrated development environment.

including designing the program to complete the illumination acquisition and setting the ESP8266 module to operate in the appropriate mode to connect to the cloud platform and transfer the data. For the programming in this paper, the FreeRTOS real-time operating system was chosen as the basis for the programming. FreeRTOS real-time operating system is free and highly real-time, with a compact kernel and open-source source code. The FreeRTOS operating system is based on a task, which is a program entity that completes a segment for a specific purpose, to complete the overall system program design. And the design of the overall system is completed by switching between the priority of each task and the control of the four task states. The state transitions between the various task states of the FreeRTOS real-time operating system are shown in Figure 7.

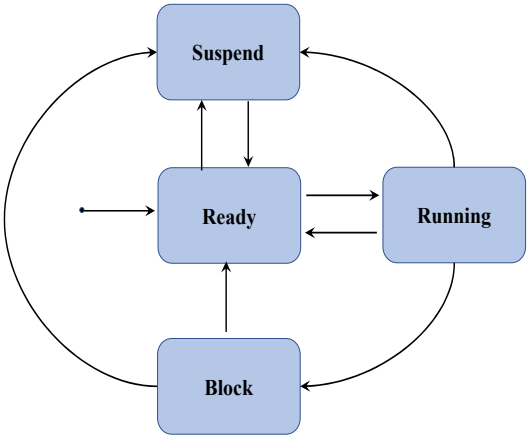

Fig. 7 Task state transition diagram

As shown in Figure 7, tasks in the FreeRTOS operating system are divided into four states, called Ready, Block, Running, and Suspend. Whenever a task is created successfully, it is automatically put in the ready state, and if the current task has a higher priority than the running task, it enters the running state, but if the priority of the current task is not higher than the priority of the running task, the current task will enter the ready state. When a task in the running state calls the function associated with vTaskDelay(), the task switches to the blocking state. A task in a blocking state will not be able to execute and be called again, and it will only end up in a blocking state when the blocking condition is met, i.e. when the Event time in the diagram occurs. And in the FreeRTOS operating system, of all the tasks in the ready state, the task with the highest priority goes into the running state. In addition, when the vTaskSuspend() function is called, the task will be converted to a pending state and the pending task will not be scheduled indefinitely, If the task is rescheduled, it can only be unmounted with the vTaskResume() function. The program flow diagram of the illumination acquisition system proposed in this paper is shown in Figure 8.

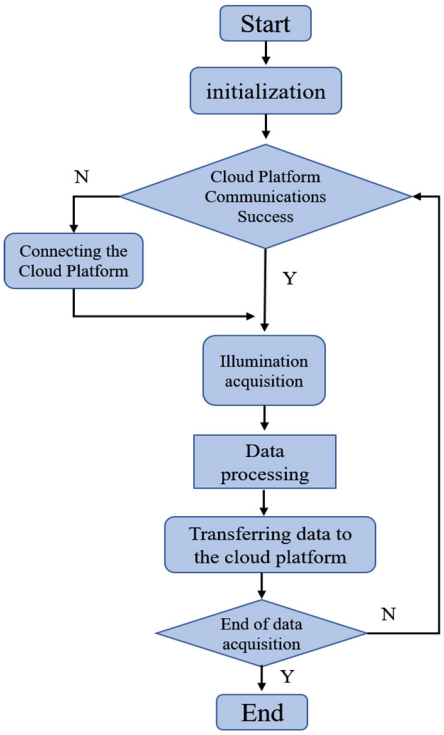

Figure.8 Illumination acquisition flow chart

WiFi-based wireless data transmission also requires data to be sent and received according to specific protocol rules. The illumination collection system proposed in the paper is based on the MQTT protocol to complete the connection to the cloud platform for data transfer. The MQTT protocol is a proxy-based publish/subscribe messaging protocol, which uses TCP/IP to provide network connectivity and maintains long TCP connections via heartbeat packets to enable real-time message pushing (Zhang, Lin, Deng 2019). The MQTT protocol is based on a client-server model with three main identities: publisher, server, and subscriber. The publisher of a message can also be the subscriber of the message, and the server acts as a relay platform for the messages.

The OneNET cloud platform is chosen as the system access platform in this paper, which is built for China Mobile IoT. The cloud platform also provides a diverse range of APIs and comprehensive development tools to enable real-time device messaging, routing and other functions, including MQTT, EDP, HTTP, and other protocol access. At the same time, the cloud platform also provides data streaming and analysis capabilities, making it easier to call data streams, simplifying the development process and reducing operational costs. In addition, the OneNET platform also offers an interface presentation and data storage and forwarding capabilities. Developers can also choose their own display components according to the characteristics of their products, and upload data in a way that supports the display of patterns and icons in the area of its page display. In addition to what has been mentioned above, developers can design and implement the monitoring interface of the upper computer directly in the cloud.

3.3 Construction of The Illumination Acquisition Platform

In this paper, the HUBSON ZINO2+ UAV was chosen as the platform for illumination acquisition. The UAV is a professional-grade UAV that can hover accurately and stably both indoors and outdoors, and it can carry heavy loads up to 500g. In addition, the UAV supports multiple flight mode settings, variable speed flight and constant speed flight, and the UAV also provides real-time feedback and records the distance and altitude of a single flight on both the mobile app and the remote control. Based on these functions, the UAV facilitates the measurement of experimental illumination and the calculation of the UAV's position.

Due to the weight limit of the UAV and the fact that the module needs to be mounted above the UAV to collect illumination, the actual size and weight of the hardware system were therefore designed to fit onto the UAV platform without compromising the stability of the UAV in flight. The module hardware is built and installed as shown in Figure 9.

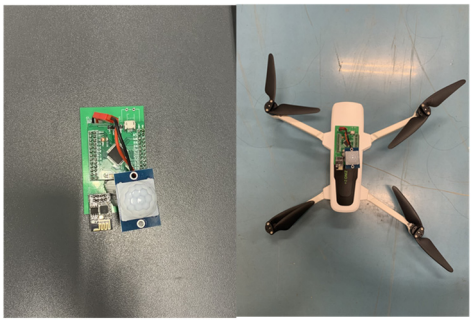

Figure. 9 Module hardware design and installation

As shown in Figure 9, the illuminance acquisition module consists of an illuminance acquisition module with spherical cosine correction, a WiFi wireless data transmission module, an STM32F103RCT6 data processing module, and a lithium battery power supply. During the actual illuminance measurement, it is fixed above the UAV for illuminance acquisition to avoid the effect of occlusion on the illuminance measurement.

4 MEASUREMENT METHOD

The HUBSAN ZINO2+ UAV used in this experiment has an optical flow positioning function, which is mainly used to determine the position information of the measurement system by using its optical flow navigation system for high-precision positioning indoors. The optical flow navigation system is a positioning method that has been used more often in UAV positioning and control systems in recent years. The method is to solve the problem of how to perform UAV attitude measurement and positioning in indoor or GPS signal-loss environments, in order to continuously broaden the application scenarios of UAVs. UAV optical flow localization is a vision-based indoor localization technique, mainly using the vSLAM technology to build a map of the indoor environment through SLAM technology (Wei 2016).

4.1 Location Determination

When the UAV is flying indoors, the image captured by the camera is matched with the image in the map library to derive information on the location of the UAV indoors (Xu 2017). The HUBSAN ZINO2+ UAV also has a camera mounted on the bottom of the drone for optical flow positioning.

Fig. 10 optical flow positioning camera of UAV

The UAV optical flow locating camera is located at the end of the tail, as shown in Figure 10. In the process of indoor positioning, the speed information of the UAV can be obtained by analyzing the acquisition of two consecutive frames of image information using the optical flow algorithm and calculating the displacement between the two frames. And the speed information can be used to control the UAV and achieve a spotting effect (Xue 2017). The basis for the implementation of the UAV optical flow algorithm is the establishment of the optical flow constraint equations under the assumptions. Firstly, the luminance is constant between frames when the target is moving; and secondly, the target moves with a small displacement. Based on these two points, the fundamental constraint equation for optical flow can be derived. Assuming that the coordinates of the image that the UAV collects during the flight is *(x,y)* and the grayscale value of the image is *I(x,y,t)*, after dt time, the image has moved a distance of *(dx,dy)* to reach the next frame. If the brightness between frames remains constant when the target is in motion, the equation below can be given:

$$I(x, y, t) = I(x + dx, y + dy, t + dt) \tag{1}$$

The Taylor expansion of equation (1) can be derived by rounding off the second order infinitesimal term if each movement produces only a small displacement. So, equation (2) can be gotten.

$$I(x, y, t) + \frac{\partial I}{\partial y} dx + \frac{\partial I}{\partial y} dy + \frac{\partial I}{\partial t} dt = I(x, y, t) \tag{2}$$

And then divide both sides of the equation by dt at the same time. In this way, equation (3) can be led to.

$$\frac{\partial I}{\partial x}\frac{dx}{dt}+\frac{\partial I}{\partial y}\frac{dy}{dt}+\frac{\partial I}{\partial t}=0 \tag{3}$$

Replacing the velocity vectors of the optical flow along the x- and y-axes with u, v, respectively, the final equation is as follows;

$$\frac{\partial I}{\partial x}u+\frac{\partial I}{\partial y}v+\frac{\partial I}{\partial t}=0 \tag{4}$$

Equation (4) is the optical flow constraint equation, where *(u,v)* denotes the optical flow value. The partial derivative of *(x,y,t)*, which can be obtained from the image data. Based on equation (4), four major classes of gradient-based, phase-based, region-based matching, and energy-based optical flow models have been proposed, respectively. The above models are used to improve the application of optical flow positioning in practical operating systems, to address the limitations of the optical flow constraint equation in practical applications, and to achieve high accuracy indoor positioning.

4.2 Illuminance measurement experiments

The actual measurement process is based on the center measurement method, with measurement points marked at 1.5m intervals.

Fig. 11 Experimental scene construction

As shown in Figure 11, at the realization site, the live picture from the UAV camera is used to assist in locating the marker point for illumination collection, and the UAV is hovered over the marker point for 50 seconds to collect illumination data from that point. The acquired illumination data is uploaded to the OneNET cloud platform for display.

Figure. 12 Cloud platform showing collected illumination data

As shown in Figure 12, the cloud platform can display the illuminance value of the current illuminance marker point location in real time. The range of illuminance values is indicated by the different colors in the display, so that the magnitude of the value and the change in illuminance can be felt more visually. As shown in Figure 13 the illuminance value is 1017lx, and the maximum value displayed at the same time can be further adjusted according to the actual situation. During the illumination measurement, the UAV hovers at each position for 50 seconds and acquires 10 data at each position. Based on the principle of least squares, the illuminance value of the point can be calculated. The least squares method estimates the model in such a way that the sum of squares of the errors is minimized, which is closer to the true situation. The basic principle of least squares is shown in Figure 13.

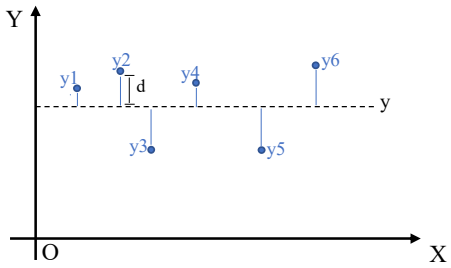

Fig. 13 Schematic diagram of the basic principle of least squares

As shown in Figure 13, there are observations of *yi* in the least squares method and suppose the true value is y. Make the distance of the observed value from the line parallel to the x-axis where the true value lies be *d*, and *d* is also the error between the true value and the observed value. As shown in equation (5).

$$d = | y - y_i | \tag{5}$$

In practical calculations, as absolute values are more cumbersome to calculate, the error between the observed value and the true value can be expressed as a square instead of an absolute value. At the same time, the sum of squares of the errors between each observation and the true value is expressed in terms of L, which gives equation (6).

$$L = \sum (y - y_i)^2 \tag{6}$$

According to equation (6), the *y* that allows the minimum value of *L* to be obtained is the true value required by the least squares method. For a quadratic function, the point at which its derivative is zero corresponds to the point of its minimum value. This leads to equation (7).

$$\frac{d}{dy} L = \frac{d}{dy} \sum (y - y_i)^2 = 2 \sum (y - y_i) = 0 \tag{7}$$

The y-value obtained by solving equation (7) is the illuminance value at the corresponding point, and it is also the arithmetic mean of the resulting data.

During the illuminance measurement process, the cloud platform is equipped with a real-time curve plotting function for real-time monitoring of the illuminance values at the collection points. Based on the inverse square law of illuminance distribution, the difference in illuminance values around the same measurement point is small, which is used to determine whether the drone is offsetting the measurement point when hovering.

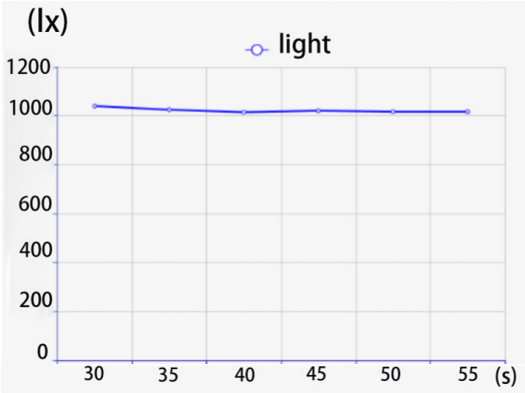

Figure .14 Cloud platform plots illumination line graphs in real time

As shown in Figure 14, the vertical axis represents the illuminance measurement value in lx, and the horizontal axis represents the illuminance measurement time with an interval of 5 seconds. Based on the curve changes, it can be seen that the illuminance values change smoothly over a 20-second time period and that the UAV makes stable illuminance measurements of the marked measurement points.

5 CONCLUTIONS

In this paper, we have built a stadium illuminance measurement system, which takes advantage of the convenience of flying drones, combined with a widely used optical flow positioning function, illumination sensors, WIFI data transmission, and a cloud platform. The system collects and uploads data at 5-second intervals with an accuracy of 1lx, using the UAV optical flow positioning function. The UAV is operated indoors to make spot measurements of illuminance more accurate. Based on the real-time feedback data from the mobile phone app, the UAV position information is obtained, and a comprehensive representation of illumination information and position information is obtained. Experiments have shown that the positioning error is 0.1m when using the UAV for indoor illumination collection. In the next step of research, the measurement system will be further improved to measure vertical illuminance under different environmental requirements of the stadium and to explore the detailed light flow distribution and three-dimensional representation of illuminance in stadiums.

ACKNOWLEDGES: This work was supported by the following: 2019 Industry Standardization Project of the Ministry of Culture and Tourism (Grant No. WH2019-19), Cooperation research project between Dalian Polytechnic University and CQC Standard (Shanghai) Testing Technology Co.,Ltd.

REFERENCES

[1] Ao Rui-Gui, Yan Xiao-Hui, Xu Shi-Guo. (2021). Research on water quality detection method based on UAV multispectral point cloud data and MGGP artificial intelligence algorithm. J. Water Resources Planning and Design, (11):5.

[2] Bendig J, Yu K, Aasen H, et al. (2015). Combining UAV-based plant height from crop surface models, visible, and near-infrared vegetation indices for biomass monitoring in barley. J. International Journal of Applied Earth Observation & Geoinformation, 39:79-87.

[3] Darren T, Arko L, Christopher W. (2012). An Automated Technique for Generating Georectified Mosaics from Ultra-High Resolution Unmanned Aerial Vehicle (UAV) Imagery, Based on Structure from Motion (SfM) Point Clouds. J. Remote Sensing, 4(5):1392-1410.

[4] Deschambault O, Gherbi A, Legare C. (2017). Efficient implementation of the MQTT protocol for embedded systems. J. Journal of Information Processing Systems, 13(1): 26

[5] Deschambault O, Gherbi A, Legare C. (2017). Efficient implementation of the MQTT protocol for embedded systems. J. Journal of Information Processing Systems, 13(1): 26－39

[6] Guo M, Sun M X, Huang M. (2021). High-precision measurement of oversized steel structures by fusing LIDAR and UAV. J. Opt. Precision Eng. 9(5):10.

[7] Li Binghua, Chang Hao, Wang Cheng, et al. (2020). An overview and analysis of the key points of venue lighting for the Winter Olympics. J. Journal of Lighting Engineering, 31(4):7

[8] Maemura T, Nakura K, Suzuki H, et al. 2017. Preliminary study of illumination distribution measurement making use of quadcopter-examination of accuracy and drawing of illumination distribution. *The 11th Asian Forum on Graphic Science.*

[9] Xie L, Xu J, Zhang R. (2018). Throughput Maximization for UAV-Enabled Wireless Powered Communication Networks. J. IEEE Internet of Things Journal, 1-1.

[10] Xue Yuan. (2019). Research on indoor positioning technology of UAV based on optical flow. P. The Nanjing University of Aeronautics and Astronautics.

[11] Xu Duo (2017). Research on indoor positioning of quadrotor UAV based on visual SLAM algorithm. P. Harbin Institute of Technology.

[12] Yao Mengming. (2012). Sports lighting design of the National Stadium (Bird's Nest). J. Journal of Lighting Engineering, 23(1):11. (in Chinese)

[13] Yu Ying, Cui Zihao, Chen Xiaoxiao. (2019). Study on the illuminance distribution and lighting scheme design of the venues of the "Fourteen Games" .J/OL. Journal of Xi'an University of Architecture and Technology.

[14] YANG Wang, FAN Zhenyu, WU Fan. (2019). Design of wireless sensing network based on 6LoWPAN and MQTT. J. Journal of National University of Defense Technology, 41(1):8.

[15] HAO Taifei, LI Hanchen, ZHANG Gang. (2019). Ultraviolet detection and localization of power line discharges by unmanned aircraft inspection. J. Opt. Precision Eng. 27(11):9.

[16] Zhang H, Lin W, Deng R. (2019) Design of IoT digital control DC voltage source based on ESP8266 WiFi module. J. Modern Electronics Technique.

[17] Wei Qingtong. (2016). SLAM-based quadrotor UAV localization and control in the indoor environment. P. Nanjing University of Aeronautics and Astronautics.